



## RESEARCH ARTICLE

WILEY

# Associations between cortical $\beta$ -amyloid burden, fornix microstructure and cognitive processing of faces, places, bodies and other visual objects in early Alzheimer's disease

José Bourbon-Teles<sup>1,2,3</sup> | Lília Jorge<sup>2,3</sup> | Nádia Canário<sup>2,3</sup> | Ricardo Martins<sup>2</sup>  | Isabel Santana<sup>4</sup> | Miguel Castelo-Branco<sup>2,3</sup> 

<sup>1</sup>HEI-Lab, Lusófona University, Lisbon, Portugal

<sup>2</sup>Coimbra Institute for Biomedical Imaging and Translational Research (CIBIT), Institute for Nuclear Sciences Applied to Health (ICNAS), University of Coimbra, Coimbra, Portugal

<sup>3</sup>Faculty of Medicine, University of Coimbra, Coimbra, Portugal

<sup>4</sup>Department of Neurology, Coimbra University Hospital, Coimbra, Portugal

## Correspondence

Miguel Castelo-Branco, Coimbra Institute for Biomedical Imaging and Translational Research (CIBIT), Institute for Nuclear Sciences Applied to Health (ICNAS), University of Coimbra, Coimbra, Portugal.  
Email: [mcbbranco@fmed.uc.pt](mailto:mcbbranco@fmed.uc.pt)

## Funding information

Fundação para a Ciência e a Tecnologia, Grant/Award Numbers: BIGDATIMAGE, CENTRO-01-0145-FEDER-000016, FCT/DSAIPA/DS/0041/2020, FCT/UIDB/4950, FCT/UIDP/4950, POCI-01-0145-FEDER-016428, PTDC/PSI-GER/1326/2020

## Abstract

Using two imaging modalities, that is, Pittsburgh compound B (PiB) positron emission tomography (PET) and diffusion tensor imaging (DTI) the present study tested associations between cortical amyloid-beta ( $A\beta$ ) burden and fornix microstructural changes with cognitive deficits in early Alzheimer's disease (AD), namely deficits in working memory (1-back) processing of visual object categories (faces, places, objects, bodies and verbal material). Second, we examined cortical  $A\beta$  associations with fornix microstructure. Seventeen early AD patients and 17 healthy-matched controls were included. Constrained spherical deconvolution-based tractography was used to segment the fornix and a control tract the central branch of the superior longitudinal fasciculus (CB-SLF) previously implicated in working memory processes. Standard uptake value ratios (SUVR) of  $A\beta$  were extracted from 45 cortical/subcortical regions from the AAL atlas and subject to principal component analysis for data reduction. Patients exhibited (i) impairments in cognitive performance (ii) reductions in fornix fractional anisotropy (FA) and (iii) increases in a component that loaded highly on cortical  $A\beta$ . There were no group differences in CB-SLF FA and in a component loading highly on subcortical  $A\beta$ . Partial correlation analysis in the patient group showed (i) positive associations between fornix FA and performance for all the visual object categories and (ii) a negative association between the cortical  $A\beta$  component and performance for the object categories but not for the remaining classes of visual stimuli. A subsequent analysis showed a positive association between overall cognition (performance across distinct 1-back task conditions) with fornix FA but no association with cortical  $A\beta$  burden, in keeping with influential accounts on early onset AD. This indicates that the fornix degenerates early in AD and contributes to deficits in working memory processing of visual object categories; though it is also important to acknowledge the importance of prospective longitudinal studies with larger samples. Overall, the effect sizes of fornical degeneration on visual working memory appeared stronger than the ones related to amyloid burden.

## KEYWORDS

Alzheimer's disease, amyloid, cognition, fornix, object processing

## 1 | INTRODUCTION

According to an influential model of early onset Alzheimer's disease (AD), the amyloid cascade hypothesis proposes that the aggregation of amyloid-beta ( $A\beta$ ) plaques trigger subsequent pathological events including the formation of neurofibrillary tangles, loss of synapses, neurons and their axons (Hardy & Allsop, 1991; Jorge et al., 2021; Reitz, 2012).

It has long been established that specific structures within the medial temporal lobes (MTL) are particularly vulnerable to AD and include the hippocampus, entorhinal cortex and the parahippocampal gyrus (Desikan et al., 2009; Devanand et al., 2012; Frisoni et al., 2010). Most notably, neurodegeneration within gray matter MTL structures have long been thought as responsible for the memory deficits observed in the early course of AD (de Toledo-Morrell et al., 2000; Köhler et al., 1998; Petersen et al., 2000; Sperling et al., 2010).

More recently, studies have also focused on the brain white matter (Acosta-Cabronero & Nestor, 2014; Huang et al., 2012). The fornix is a prominent limbic tract that contains both afferent and efferent pathways connecting the hippocampus with a number of subcortical and cortical structures including the mammillary bodies, the anterior thalamus and portions of the prefrontal cortex (Aggleton, 2012; Aggleton et al., 2010). Recent studies suggest microstructural changes to the fornix to predict conversion from normal aging to mild cognitive impairment (MCI) (Fletcher et al., 2013; Lee et al., 2012; Zhuang et al., 2013) and from MCI to early AD dementia (Lee et al., 2012; Mielke et al., 2012) and to even precede gray matter hippocampal volume loss during healthy aging (Metzler-Baddeley et al., 2019). Furthermore, the degree of fornix microstructural damage has been associated with the degree of memory impairment in early AD (Douet & Chang, 2015; Mielke et al., 2012; Oishi & Lyketsos, 2014). Thus, given the increasing number of recent studies implicating fornix changes in the early pathology of AD, further research is warranted for a better understanding of its contributions to the early disease process, for example, to the decline in cognitive functions beyond memory (Douet & Chang, 2015; Oishi & Lyketsos, 2014).

In the present study, we tested contributions of cortical  $A\beta$  burden and/or fornix microstructural changes to cognitive deficits in early AD, namely to impairments in visual object category processing (i.e., faces, places, objects, bodies and verbal material) as measured by 1-back working memory tasks. A secondary question tested whether cortical  $A\beta$  burden is negatively associated with microstructural characteristics of the fornix.

The role of the fornix in cognition has been established beyond processes related to long-term memory (e.g., in working memory) in animal studies. In rodents, fornix lesions have been shown to impair successful working memory performance in delayed match/non-match to sample tasks and radial-arm maze tasks (Aggleton et al., 1992; Bubb et al., 2018; Cassaday & Rawlins, 1995; Galani et al., 2002; Markowska et al., 1989; Sziklas & Petrides, 2002). In addition, there is evidence supporting hippocampal involvement (which is known to be structurally related to the fornix) in the online

maintenance of visual information at short-delay periods (Hannula et al., 2006; Kantarci, 2014; Leszczynski, 2011; Olson et al., 2006; Warren et al., 2012, 2014) which is also in keeping with an integrative role of the hippocampus beyond long-lasting memory.

In addition, deficits in visual working memory functions have been reported in the AD patient population and commonly concern difficulties in processing a variety of features (e.g., color, orientation or location) of the stimuli to be held in memory (e.g., Zokaei & Husain, 2019). Here, we tested AD-associated deficits in the processing everyday visual object category information into working memory and a potential fornix predictive role.

While tractography based on the single diffusion tensor model has been shown to provide anatomical plausible reconstructions of tracts located within regions with highly coherent fiber orientations it fails to provide reliable trajectories of fibers with a considerable number of crossing fiber populations such as in the case of the fornix (Pierpaoli et al., 2001). In order to overcome this limitation, constrained spherical deconvolution (CSD)-based tractography which estimates a white matter (WM) fiber orientation distribution function (fODF) in each voxel was chosen as the appropriate method to segment the fornix and other fiber tracts (Tournier et al., 2004, 2007). In addition, we studied measures of fornix fractional anisotropy (FA) which appear to be rather robust against partial volume contaminations driven by cerebrospinal (CSF) fluid (e.g., Metzler-Baddeley et al., 2012).

To test for specific associations between cortical  $A\beta$  burden/fornix microstructural changes and cognitive decline the statistical analysis was controlled for measures of FA in the central branch of the superior longitudinal fasciculus (CB-SLF) because of its previous associations with working memory/attention control processes (Bourbon-Teles et al., 2021; Thiebaut de Schotten et al., 2011) and subcortical  $A\beta$  burden following previous observations supporting elevated  $A\beta$  depositions to occur predominantly in the cortex in comparison to subcortical nuclei in preclinical AD (e.g., Edmonds et al., 2016).

Following influential accounts on early onset AD, we hypothesized that fornix microstructural changes should be better predictive of the cognitive and clinical symptoms in comparison with manifest cortical  $A\beta$  burden (Berron et al., 2020; Hanseeuw et al., 2019; Hardy & Allsop, 1991; Marks et al., 2017; Svenningsson et al., 2019).

## 2 | METHODS

### 2.1 | Participants

For this study, 34 participants were selected to take part (sample size based on Jorge et al., 2021). Post hoc power estimates were not used because are generally variable in the range of practical interest and can be very different from the true power (Zhang et al., 2019). All participants gave their written informed consent, approved by the Ethics Committee of the University of Coimbra. A total of 17 patients with early AD (eight females and nine males, mean age = 66.47 years) were recruited at the Neurology department of the Centro Hospitalar e

**TABLE 1** CSF biomarker levels of AD patients

	A $\beta_{1-42}$ (n = 17)	A $\beta_{42}/A\beta_{40}$ (n = 14)	Tau (n = 17)	pTau (n = 17)	Tau/A $\beta_{42}$ (n = 17)	A $\beta_{42}/p$ Tau (n = 17)
Mean	510.94	0.057	445.64	63.15	0.98	9.23
SD	215	0.021	246.80	24.36	0.52	6.28

Note: Normal values as follow: A $\beta_{1-42}$  > 580 pg/ml; A $\beta_{42}/A\beta_{40}$  > 0.068; Tau <250 pg/ml; pTau (181) < 37 pg/ml; Tau/A $\beta_{42}$  < 0.40; A $\beta_{42}/p$ Tau >15.8. Abbreviation: SD, standard deviation.

Universitário de Coimbra (CHUC). We recruited patients with a probable diagnosis of AD as supported by biological markers (CSF or Pittsburgh compound B-positron emission tomography [PiB-PET]) and in mild stages of the disease as supported by the global staging scale Clinical Dementia Rating (i.e., CDR = 1) (Morris, 1993).

The selected criteria for diagnosis of AD was based on the Diagnostic and Statistical Manual of Mental Disorders–fourth edition (DSM-IVTR) and the National Institute of Neurological and Communicative Disorders and Stroke-Alzheimer's Disease and Related Disorders (NINCDS-ADRDA) (McKhann et al., 2011). Extensive neuropsychological evaluation was conducted with the Mini-Mental State Examination (MMSE) with Portuguese normative data (Folstein et al., 1975; Freitas et al., 2015), with the Montreal Cognitive Assessment (MoCA) test (Freitas et al., 2013; Nasreddine et al., 2005) and with a comprehensive neuropsychological battery with normative data for the Portuguese population (BLAD) exploring memory and other cognitive domains (Guerreiro, 1998).

Subcortical volumetric analysis was conducted and confirmed hippocampal atrophy in the patient group versus controls (patients mean hippocampal volume = 4326 mm<sup>3</sup>, controls mean hippocampal volume = 5139 mm<sup>3</sup>,  $p = .005$ ) in support of a probable AD diagnosis. CSF biomarkers levels of A $\beta_{1-42}$ , A $\beta_{42}/A\beta_{40}$ , tau and pTau181 were also consisted with a clinical diagnosis of AD (see Table 1). The cut-off values used in our laboratory and applied for the current study were as follow: 580 pg/ml for A $\beta_{1-42}$ , 0.068 for A $\beta_{42}/A\beta_{40}$ , 250 pg/ml for tau and 37 pg/ml for pTau181 (Table 1).

We considered patients that were on stable medication and without significant acute events. Criteria of exclusion included: ophthalmological comorbidities, neurological/psychiatric conditions other than AD and MRI demonstration of significant vascular burden (large cortico-subcortical infarct; extensive subcortical WM lesions superior to 25%; uni- or bilateral thalamic lacune; lacune in head of caudate nucleus; more than two lacunes) (McKhann et al., 2011).

A selected control group of 17 participants (nine males and eight females, mean age = 65.24 years) comprised age, sex and education-matched subjects from the community. The controls had no history of cognitive deterioration, neurological or acquired CNS disorders, traumatic brain injury, psychiatric disorders, or alcohol abuse or any other substance abuse. The control individuals were not subject to any medication that could have interfered with the study. Furthermore, they showed no evidence of significant memory complaints (as assessed by a subjective memory complaint [SMC] scale) (Ginó et al., 2008; Schmand et al., 1996), exhibited a normal general cognitive function (assessed by the MoCA test) (Freitas et al., 2013; Nasreddine et al., 2005), preserved daily living activities (assessed by the Lawton &

Brody scale) (Lawton & Brody, 1969; Madureira & Verdelho, 2008) and showed no evidence of depressive symptoms (measured by the Geriatric Depression Scale) (Barreto et al., 2008; Yesavage et al., 1982).

All participants from the current study underwent a comprehensive ophthalmological evaluation to guarantee the absence of any visual complications. Visual assessment comprised visual acuity assessment with Snellen chart, ocular tension (Goldmann applanation tonometer), slit lamp biomicroscopy, and optical coherence tomography (OCT) imaging. Only subjects with normal or corrected to normal vision were considered to the present study, that is, with visual acuity  $\geq 8/10$ , with refractor error between  $\pm 5$  dioptres, with intraocular pressure  $\leq 21$  mmHg, and without apparent alterations of the optic disc or macula.

## 2.2 | Cognitive assessment

Cognitive performance (i.e., working memory) was assessed with 1-back-tasks for the following stimulus categories: faces, objects, bodies, places and verbal material each of them comprising three subcategories (see, e.g., Figure 1a). All of the stimulus categories consisted of grayscale images. The faces category was composed of young, middle and old faces, obtained from the FACES database (Ebner et al., 2010). The objects category comprised tools, cars and chairs subcategories and were all obtained from publicly available sources. The bodies' category was represented by faceless bodies, body shape silhouettes, hands and feet. The faceless bodies images were taken from the Bochum Emotional Stimulus Set database (Thoma et al., 2013), and hands and feet were selected from publicly available images that were obtained online. Body shape silhouettes images were generated with a customized code in MATLAB R2014a (MathWorks, Natick). The places category comprised landscapes, buildings and skylines and were obtained from both online searches and a database of the computational visual cognition laboratory (Oliva & Torralba, 2001) (<http://cvcl.mit.edu/database.htm>). The verbal material was composed by words, pseudo and non-words and provided as a courtesy from the database of Universidade Católica Portuguesa. Images from each category were further equalized in terms of luminance with the SHINE toolbox (Willenbockel et al., 2010). This procedure calculates a globally equalized luminance based on the average of the image input matrices. In order for the Shine procedure to be correct, a verified luminance-corrected matrix needs to be calculated based on the SpectroColorimeter PR-650 (Canário et al., 2016).

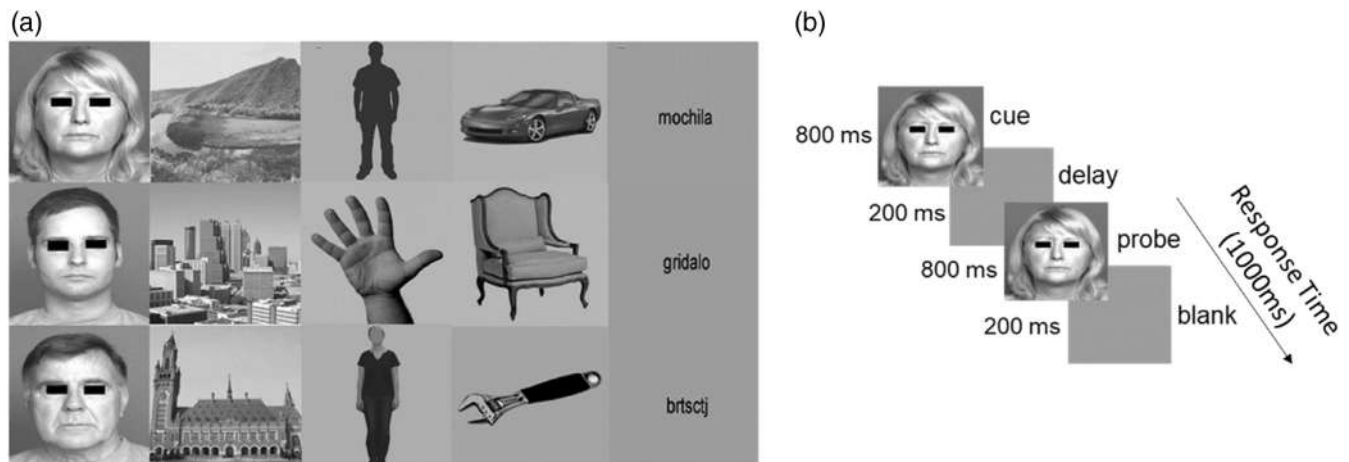


**FIGURE 1** (a) Examples of faces, places, bodies, objects and verbal subcategories of stimuli (b) illustration of the 1-back working memory tasks as follow: Cue (800 ms) + delay (200 ms) + probe (800 ms) + blank screen (200 ms). Participants were asked to press a button every time cue and probe matched and to abstain from pressing any button whenever cue and probe did not match. Note that individual stimulus could either serve as cue and/or probe. ms, milliseconds

The stimulus categories were tested in two different runs (versions A and B) and presented randomly in a block-design paradigm. Individual runs were composed by 18 blocks and lasted for 9 min and 17 s. Each block had a duration of 20 s and was composed by 20 images that always belonged to the same subcategory of stimuli (e.g., regarding the face categories a single block would always be composed of either just young faces, middle aged faces, or old faces). Within each block there were a total of four match trials and 16 non-match trials. In addition, each block was separated by a 10 s interval filled with a uniform grayscale image with no stimulus.

Please note that scrambled versions of visual object categories were also tested in the current experiment; however, since these represent meaningless abstract material they were not considered for the present study.

During the 1-back tasks, individual images were presented for 800 ms with a 200 ms interval and participants were requested to press a button with their dominant hand every time the image being presented was the same that had been presented before (see Figure 1b). The order of blocks was presented in a pseudo-randomized fashion. There were four repetitions of images within each block. Before starting the actual experiment, subjects performed a brief training session in order to guarantee that they understood the task demands and to be familiarized with the stimuli.

Visual stimuli were presented using Presentation 17.1 software (Neurobehavioral systems) on a uniformly black background. Stimuli were presented using a Fujitsu PC (1920 × 1080) onto an LCD screen. The image size used to build the stimuli was 544 × 544 pixels and subtended approximately 11° × 11° of visual field.

Finally, measures of mean response accuracy in the 1-back tasks were extracted for each individual participant.

### 2.3 | MRI data acquisition

MRI data were acquired in a 3 Tesla Siemens Magnetom TrioTim scanner (Erlangen, Germany) at the Institute of Nuclear Sciences Applied to Health (ICNAS) using a 12-channel birdcage head coil. The session started with one 3D anatomical MPRAGE (rapid gradient-echo) sequence T1-weighted with a  $1.0 \times 1.0 \times 1.0$  mm voxel resolution, repetition time (TR) 2530 ms, echo time (TE) 3.42 ms, field of view (FOV)  $256 \times 256$  mm. The MPRAGE sequence comprised 176 slices, a flip angle of 7° and an inversion time of 1100 ms. The protocol also included a diffusion tensor imaging (DTI) sequence with the following parameters: TR/TE = 7800/90 ms, number of excitations = 1, matrix =  $96 \times 96 \times 63$  contiguous axial slices, isotropic voxel resolution =  $2 \times 2 \times 2$  mm<sup>3</sup>, bandwidth = 1628 Hz/pixel, echo spacing = 0.72 ms, 63 noncollinear directions, one scan without diffusion weighting ( $b = 0$  s/mm<sup>2</sup>,  $b_0$ ), ( $b$ -value = 1000 s/mm<sup>2</sup>).

### 2.4 | DTI data processing and tractography

The diffusion-weighted MRI images were corrected for subject motion, eddy-current induced distortions and EPI deformations by registering each image volume to the high-resolution T1-weighted anatomical images (Irfanoglu et al., 2012; Soares et al., 2013) with appropriate reorientation of the encoding vectors (Leemans & Jones, 2009) in ExploreDTI (Version 4.8.6) (Leemans et al., 2009). The fornix and the CB-SLF were segmented using CSD-based deterministic tractography (Jeurissen et al., 2011; Tourmier et al., 2004, 2007) with the following parameters: uniform whole-brain seeding with 2 mm resolution, step size 1 mm, fiber orientation distribution threshold of 0.1 and maximum angle deviation of 30°.

Three-dimensional fiber reconstructions were made by applying waypoint ROI gates (“AND,” “SEED” and “NOT” gates following

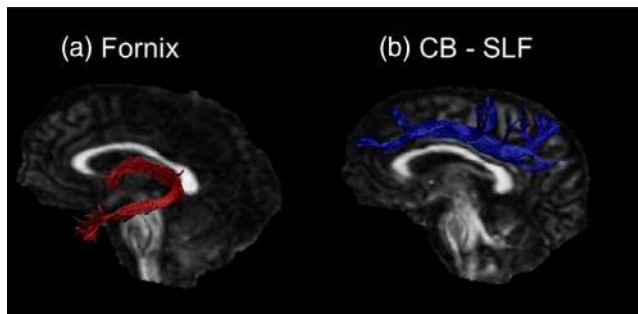


**FIGURE 2** Depicts sagittal views of (a) the fornix and (b) the central branch of the superior longitudinal fasciculus (CB-SLF)

Boolean logic) to isolate specific tracts from the whole brain CSD-based tractography data.

The reconstruction of the fornix (in Figure 2a) followed the protocol by Metzler-Baddeley et al. (2011). In short, a seed ROI was placed on the coronal slice around the area where the anterior pillars enter into the main body of the fornix. An AND ROI was placed on the axial plane encompassing the crush of the fornix in both hemispheres around the inferior part of the splenium of the corpus callosum. Then, NOT gates were drawn around areas that are not part of the fornix shape.

Further, as specified earlier in order to assess for specific associations between fornix microstructure and cognitive performance we controlled for CB-SLF microstructure (because of its previous associations with working memory/attention control functions) in the statistical analysis. The reconstruction of the CB-SLF (in Figure 2b) followed the protocol by Thiebaut de Schotten et al., 2011. In essence, a coronal seed ROI was placed at the level of the posterior commissure around the parietal lobe and an AND ROI was placed around the middle frontal gyrus. Further, NOT gates were drawn around areas that are not part of the CB-SLF shape. Measures of CB-SLF FA were collapsed/averaged across both hemispheres and computed for each individual participant.

## 2.5 | PET acquisition, processing, and quantitative analysis

[11C]-PiB PET data were acquired at Institute of Nuclear Sciences Applied to Health (ICNAS), University of Coimbra, using a Philips Gemini GXL PET/CT scanner (Philips Medical Systems, Best). The participants performed a dynamic 3D PET scan of the entire brain (90 slices, 2-mm slice sampling) and a low-dose brain CT scan, for attenuation correction. The dynamic [11C]-PiB PET consists of 37 frames (total duration of 90 min:  $4 \times 15$  s +  $8 \times 30$  s +  $9 \times 60$  s +  $2 \times 180$  s +  $14 \times 300$  s). The [11C]-PiB PET acquisition started immediately after the intravenous bolus injection of approximately 555 MBq of [11C]-PiB. To minimize head movement, the patient's head was restrained with a soft elastic tape. The [11C]-PiB PET images were reconstructed to a  $128 \times 128 \times 90$  matrix, with

isotropic voxels of 2 mm width, using the LOR RAMLA algorithm (Philips PET/CT Gemini GXL) with attenuation and scatter correction.

For each participant, a sum image was obtained using all the frames of the dynamic PET. The sum image was used to estimate a rigid transformation between the [11C]-PiB PET image space and the T1 anatomical MRI space of each participant. The rigid transformation was determined using 3D Slicer software (version 4.8.1, BRAINS registration tool) (Kikinis et al., 2014). The individual MRI scans were spatially normalized to the Montreal Neurological Institute (MNI) template using DARTEL algorithm (Ashburner, 2007) in Statistical Parametric Mapping (SPM) 12 toolbox (Wellcome Trust Centre for Neuroimaging).

The voxel-level quantitative analysis of [11C]-PiB PET images was implemented in the MNI space using in-house made software (Oliveira et al., 2018), and by resampling the PET data to the MNI space applying the geometric transformations described previously. The individual [11C]-PiB standard uptake value ratio (SUVR) map was computed by summing voxel-level signal from 40 to 70 min post-injection, and dividing by the mean signal from the individual's reference region, the cerebellar gray matter (essentially the cerebellum without the cerebellar peduncles) (Price et al., 2005). For each individual participant, the mean SUVR value of 45 regions-of-interest (ROI) (averaged across hemispheres) was extracted from the individual voxel-level SUVR map in the MNI space using the anatomical automatic labelling (AAL) atlas (Tzourio-Mazoyer et al., 2002) (see Table 3) and the 3D Slicer software.

## 2.6 | Statistical analysis

All statistical analyses were carried out in IBM SPSS statistical package (version 26). Given the large number of extracted measures from the PET data we conducted a principal component analysis (PCA) based on the 45 SUVR of molecular A $\beta$  across distinct cortical/subcortical regions from the AAL atlas (Table 3). The main purpose of PCA was to identify the minimum number of uncorrelated principal components that together explained the maximum amount of variance of the molecular A $\beta$  data (Jolliffe, 1986).

Due to the relatively small sample size for PCA ( $n = 34$ ) we followed recommendations to limit the number of extracted components to a minimum (de Winter et al., 2009; Preacher & MacCallum, 2002). Given that there is no single recommended method available, we adopted the following strategy: first, we employed the SPSS default of the Kaiser criterion of including all components with an eigenvalue of  $>1$ . Second, we inspected Cattell's scree plots (Cattell, 1952) to identify the minimal number of components that accounted for most of the variability in the data. Third, we assessed each component with regard to their interpretability. We used a PCA procedure with orthogonal Varimax rotation of the component matrix. Per convention, loadings that exceeded a value of 0.5 were regarded as significant. Table 3 summarizes the component loadings for the SUVR of regional molecular A $\beta$ .



Firstly, we computed the mean accuracy scores which was simply based on the proportion of the same/correct responses, for the target events. Subsequently, the data were checked for normality with Shapiro–Wilk tests for the group of patients and healthy controls separately.

We then tested for group differences in the principal component scores (i.e., from the extracted cortical A $\beta$  and subcortical A $\beta$  components) (see Table 3), fornix microstructure and CB-SLF microstructure with independent samples *t*-tests. Group differences in cognitive performance (as measured by mean response accuracy [Acc] and mean response times [RTs]) were tested with Mann–Whitney *U* tests.

Subsequently, partial correlations were conducted to test relationships between the cortical A $\beta$  component, fornix microstructure with (i) cognitive performance for each individual 1-back task measures and (ii) overall cognitive performance measures (computed as follow: Acc faces + Acc places + Acc bodies + Acc objects + Acc verbal/5). In addition, we also tested associations between fornix FA and the cortical A $\beta$  component with partial correlations. All the statistical analysis were conducted in the patient and healthy control groups separately and the control variables included in the regression models were: age, education, sex, CB-SLF microstructure and the subcortical A $\beta$  component. Thus, these analyses allowed testing individual associations between fornix FA and/or cortical A $\beta$  burden with cognitive performance above and beyond CB-SLF FA (a WM region previously implicated in working memory/attention control functions) and subcortical A $\beta$  burden.

All statistical tests were corrected for multiple comparison errors with the Bonferroni correction with a family-wise alpha level of 5% (two-tailed) leading to a corrected *p*-value of (i)  $p \leq .025$  for two *t*-tests for molecular A $\beta$  data (ii)  $p \leq .025$  for two *t*-tests for microstructural data (iii)  $p \leq .01$  for five Mann–Whitney *U* tests concerning cognitive performance (i.e., separately for Acc and RTs scores) (iv)  $p \leq .05$  for one correlation between cortical A $\beta$  component and/or fornix FA with overall cognitive performance measures and (v)  $p \leq .05$  for one correlation between fornix FA and cortical A $\beta$  component. In addition, with regards to the analysis concerning individual associations between the cortical A $\beta$  component and/or fornix FA with individual cognitive performance measures the significance levels differed when the analysis was conducted in the patient sample and/or in the control sample. In the analysis concerning the patient data sample we performed (i) three parametric correlations between the cortical A $\beta$  component and/or fornix FA with cognitive performance measures (i.e., the mean accuracy scores for faces, places and body categories) each requiring a level of significance of  $p \leq .016$  and (ii) two non-parametric correlations between the cortical A $\beta$  component and/or fornix FA with cognitive performance measures (i.e., the mean accuracy scores for objects and verbal categories) each requiring a level of significance of  $p \leq .025$ . By comparison, with regards to the healthy control sample there were five non-parametric correlations each requiring a  $p \leq .01$  to comply with a family-wise alpha level of 5%.

### 3 | RESULTS

Patients and controls were matched for age, sex and education. Patients showed as expected reduced performance in MoCA test. Every patient had a CDR of 1, being affected by mild dementia (Table 2). With regards to performance in the BLAD test, patients showed the highest ratio of impairment in the memory domain (16/17), followed by the executive domain (12/17), language (7/17), constructive (4/17) and calculation (3/17) domains.

Part of the patient population data (i.e., DTI, PET and cognitive accuracy data) conformed to normality with exception for the mean accuracy scores for objects and verbal categories and the overall cognitive performance measures for which partial Spearman rho correlations were conducted. By comparison, for the healthy control group only the DTI and PET data conformed to normality while the cognitive accuracy data did not conform to normality for which partial Spearman rho correlations were conducted.

Finally, with regards to the cognitive RT data, in the patient sample only the mean RT scores for places and the verbal categories conformed to normality while for the control data sample all of the RT data were normally distributed.

#### 3.1 | Group differences in PET, DTI and cognitive measures

With PCA, two components were extracted that together explained 90.3% of the variability in the PET data (Table 3). The first component loaded highly predominately on cortical amyloid SUVR and it is summarized as the “cortical A $\beta$  component.” By comparison, the second component loaded highly predominantly on subcortical amyloid SUVR and it is summarized as the “subcortical A $\beta$  component” (Table 3).

Patients showed significant increases in the cortical A $\beta$  component in line with the notion that at early stages AD A $\beta$  depositions are already widespread throughout the cortex. There were no significant differences in the subcortical A $\beta$  component. Regarding DTI measures, there were significant reductions in fornix FA in the patient group. No significant differences were observed in CB-SLF FA (Table 4).

**TABLE 2** Demographics and clinical characteristics of study participants

Mean (SD)	Patients (n = 17)	Controls (n = 17)	<i>p</i> -value
Age	66.47 (6.63)	65.24 (7)	.601
Education	9.06 (6)	11.59 (5.8)	.22
Sex (F/M)	8/9	9/8	.74
MoCA	14.47 (4.51)	25 (4.5)	<.001
MMSE	23.1 (2.97)		
CDR	1	0	

Note: Data are expressed as mean (SD). The higher the scores in the MMSE and MoCA the better the performance.

Abbreviations: F, female; M, male.

**TABLE 3** Rotated component matrix of the principal component analysis of the molecular A $\beta$  data ( $n = 34$ )

Regional A $\beta$ SUVR	“Cortical A $\beta$ component”	“Subcortical A $\beta$ component”
<i>Cortical</i>		
Precentral gyrus	<b>0.909</b>	0.288
Superior frontal gyrus, dorsolateral	<b>0.893</b>	0.402
Superior frontal gyrus, orbital part	<b>0.881</b>	0.383
Middle frontal gyrus	<b>0.908</b>	0.383
Middle frontal gyrus, orbital part	<b>0.852</b>	0.424
Inferior frontal gyrus, opercular part	<b>0.908</b>	0.375
Inferior frontal gyrus, triangular part	<b>0.904</b>	0.406
Inferior frontal gyrus, orbital part	<b>0.892</b>	0.351
Rolandic operculum	<b>0.913</b>	0.352
Supplementary motor area	<b>0.919</b>	0.325
Olfactory cortex	<b>0.808</b>	0.435
Superior frontal gyrus, medial	<b>0.892</b>	0.399
Superior frontal gyrus, medial orbital	<b>0.852</b>	0.424
Gyrus rectus	<b>0.903</b>	0.364
Insula	<b>0.892</b>	0.407
Anterior cingulate and paracingulate gyri	<b>0.860</b>	0.483
Median cingulate and paracingulate gyri	<b>0.890</b>	0.415
Posterior cingulate gyrus	<b>0.656</b>	<b>0.567</b>
Parahippocampal gyrus	<b>0.625</b>	<b>0.615</b>
Calcarine fissure and surrounding cortex	<b>0.919</b>	0.088
Cuneus	<b>0.944</b>	0.065
Lingual gyrus	<b>0.926</b>	0.016
Superior occipital gyrus	<b>0.949</b>	0.095
Middle occipital gyrus	<b>0.963</b>	0.162
Inferior occipital gyrus	<b>0.961</b>	0.110
Fusiform gyrus	<b>0.931</b>	0.305
Postcentral gyrus	<b>0.927</b>	0.293
Superior parietal gyrus	<b>0.901</b>	0.328
Inferior parietal, but supramarginal and angular gyri	<b>0.881</b>	0.401
Supramarginal gyrus	<b>0.907</b>	0.384
Angular gyrus	<b>0.910</b>	0.383
Precuneus	<b>0.902</b>	0.374
Paracentral lobule	<b>0.865</b>	0.312
Heschl gyrus	<b>0.882</b>	0.374

(Continues)

**TABLE 3** (Continued)

Regional A $\beta$ SUVR	“Cortical A $\beta$ component”	“Subcortical A $\beta$ component”
Superior temporal gyrus	<b>0.904</b>	0.395
Temporal pole: superior temporal gyrus	<b>0.836</b>	0.418
Middle temporal gyrus	<b>0.944</b>	0.308
Temporal pole: middle temporal gyrus	<b>0.871</b>	0.371
Inferior temporal gyrus	<b>0.927</b>	0.329
<i>Subcortical</i>		
Hippocampus	-0.148	<b>0.809</b>
Caudate nucleus	0.147	<b>0.752</b>
Putamen	<b>0.774</b>	<b>0.576</b>
Pallidum	0.421	<b>0.684</b>
Thalamus	0.270	<b>0.826</b>
Amygdala	<b>0.657</b>	<b>0.649</b>

Note: Loadings >0.5 are highlighted in bold.

Patients also exhibited reduced cognitive performance though this was only present at the level of response accuracy but not at the level of RTs (Table 5).

### 3.2 | Partial correlations between fornix FA, cortical A $\beta$ burden and individual cognitive performance measures

There were statistically significant positive associations between fornix FA and individual cognitive performance for faces ( $r = .76$ ,  $p = .004$ ), places ( $r = .7$ ,  $p = .01$ ) and body categories ( $r = .7$ ,  $p = .01$ ). Non-parametric correlation analysis also revealed statistically significant positive associations between fornix FA and cognitive performance for objects ( $r_s = .76$ ,  $p = .004$ ) and verbal categories ( $r_s = .7$ ,  $p = .01$ ) (Figure 3a). Overall, these findings are in keeping with robust fornical contributions to short-term visual object category processing functions in early AD.

There was a trend (i.e., significant at uncorrected level) for a negative association between the cortical A $\beta$  component and cognitive performance for object categories ( $r_s = -.62$ ,  $p = .03$ ). By comparison, there were no significant associations between the cortical A $\beta$  component and cognitive performance for faces ( $r = -.35$ ,  $p = .26$ ), places ( $r = -.5$ ,  $p = .1$ ), bodies ( $r = -.53$ ,  $p = .077$ ), and verbal categories ( $r_s = -.5$ ,  $p = .06$ ) (Figure 3b).

For the control group there was a significant negative association between the cortical A $\beta$  component and cognitive performance for face categories ( $r_s = -.7$ ,  $p = .01$ ). There was also trend for a negative association between the cortical A $\beta$  component and performance for the object categories ( $r_s = -.62$ ,  $p = .03$ ). There were no other significant associations between the cortical A $\beta$  component and/or fornix FA with individual cognitive performance measures (data not shown).

Mean (SD)	Patients (n = 17)	Controls (n = 17)	p-value
<i>PET</i>			
Cortical A $\beta$ component	0.81 (0.8)	-0.81 (0.17)	<.001***
Subcortical A $\beta$ component	0.28 (1.3)	-0.28 (0.47)	.094
<i>DTI</i>			
Fornix FA	0.21 (0.03)	0.26 (0.03)	.001***
CB-SLF FA	0.56 (0.07)	0.55 (0.04)	.73

**TABLE 4** Effects of group (patients vs. controls) on PET and DTI measures

Note: Data are expressed as mean (SD).

\*\*\* $p \leq .001$ .

**TABLE 5** Effects of group (patients vs. controls) on cognitive performance measures

Mean (SD) Cognitive performance (stimulus)	Response accuracy			RTs		
	Patients (n = 17)	Controls (n = 17)	p-value	Patients (n = 17)	Controls (n = 17)	p-value
Faces	2.51 (0.9)	3.45 (0.6)	.003**	729 (260)	688 (87)	.46
Places	2.22 (1.3)	3.33 (0.9)	.004**	631 (190)	665 (92)	.69
Objects	2.16 (1.2)	3.3 (0.77)	.003**	660 (190)	664 (88)	.82
Bodies	1.96 (1.1)	3.35 (0.8)	<.001***	703 (405)	677 (96)	.62
Verbal	2.1 (1.3)	3.35 (0.9)	.002**	671 (108)	696 (95)	.66

Note: Data are expressed as mean (SD). RTs are given in ms.

\*\* $p \leq .01$ ; \*\*\* $p \leq .001$ .

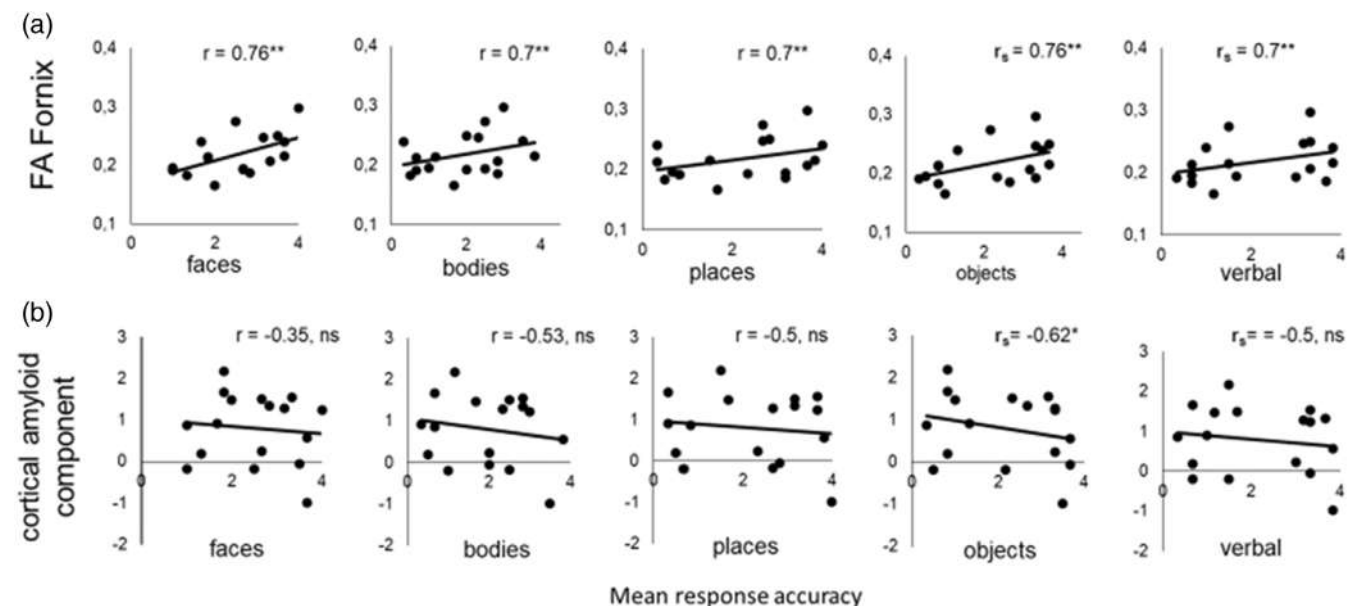


**FIGURE 3** Plots the individual correlations and coefficients (controlled for covariates of interest) between (a) fornix FA and (b) cortical A $\beta$  burden and cognitive performance for visual object categories in the patient group (n = 17). \* $p \leq .05$ , \*\* $p \leq .01$ . ns, nonsignificant

### 3.3 | Partial correlations between fornix FA, cortical A $\beta$ burden and overall cognitive performance measures

For the patient group there was a statistically significant positive association between fornix FA and overall cognitive performance

( $r_s = .82, p = .001$ ). By comparison, there was no significant association between the cortical A $\beta$  component with overall cognition ( $r_s = -.5, p = .09$ ).

For the control group there were no significant associations between fornix FA and/or the cortical A $\beta$  component with overall cognition (data not shown).



### 3.4 | Partial correlations between fornix FA and cortical A $\beta$ burden

There were no statistically significant associations between fornix FA and the cortical A $\beta$  component in the patient group ( $r = -.33, p = .3$ ). Similarly, there were also no significant associations between fornix FA and the cortical A $\beta$  component in the analysis concerning the control group ( $r = -.54, p = .07$ ).

## 4 | DISCUSSION

The main aim of the present study was to test associations between cortical A $\beta$  burden and fornix microstructural changes with cognitive deficits in patients with early AD. In particular we sought to determine if cortical A $\beta$  burden and fornix changes link to deficits in cognitive functions beyond long-lasting memories, namely to deficits in working memory processing of everyday visual object categories (i.e., faces, objects, bodies, places and verbal material). Secondly, we also exploited potential negative associations between fornix microstructure and cortical A $\beta$  amyloid in early AD patients.

Consistent with previous studies, we found that patients exhibited (i) deficits in cognitive processing, notably in terms of response accuracy (ii) impairments in fornix microstructure and (iii) significant increases in a component that loaded highly on A $\beta$  across the extensive cortex in line with the notion that at early stages AD A $\beta$  amyloid depositions are already widespread throughout the cortex (Cho et al., 2016; Edmonds et al., 2016; Jorge et al., 2021; Kensinger et al., 2003; Oishi & Lyketsos, 2014). By comparison, there were no significant effects of disease on CB-SLF microstructure and on subcortical A $\beta$  burden. Overall, these findings support the hypothesis that cortical A $\beta$  depositions and fornix changes constitute early and specific biomarkers in AD (Cho et al., 2016; Edmonds et al., 2016; Oishi & Lyketsos, 2014). With regards to our second aim, cortical A $\beta$  burden was not negatively associated with fornix FA in the AD patient group.

Subsequently, analysis at the individual predictor level indicates that fornix microstructural changes link better to the impairments in face category processing in contrast to manifest cortical A $\beta$  burden depositions in early AD. Furthermore, there were individual associations between fornix microstructure and/or cortical A $\beta$  burden with cognitive performance for the object categories, though the effects of cortical A $\beta$  burden were still lower and significant at the uncorrected level, clearly showing that the effect sizes are stronger concerning functional effects of fornical lesions in AD. Accordingly, previous research by Nichols et al., 2006 reported hippocampal activations during the maintenance of faces at short-delay periods (i.e., into working memory) and that the degree of hippocampal responses were predictive of performance in a later face recognition task. In addition, hippocampal lesions have been shown to impair working memory representations of faces and other visual information (Ezzyat & Olson, 2008; Olson et al., 2006). Moreover, research in older adults support a link between disrupted hippocampal-prefrontal connectivity

(a network supported by the fornix) and deficits in face recognition (Dennis et al., 2008; Grady et al., 1995).

Additionally, the findings reported here also support stronger contributions of fornical microstructural changes to cognitive deficits in the processing of places, bodies and verbal categories in early AD patients, in comparison to manifest cortical A $\beta$  burden. Thus, a link between fornix microstructure and place processing at this level is not surprising given the well-established roles of the fornix/hippocampus in high-level visuospatial processing abilities and place processing (Bird & Burgess, 2008; Buckley et al., 2004; Gaffan, 1994; Hodgetts et al., 2015; Postans et al., 2014; Wilson et al., 2008). For instance, studies in non-human primates have shown that fornix transections impair learning of object-in-place associations and conjunctions of spatial features both of which represent necessary attributes for place processing and representation (Buckley et al., 2004; Gaffan, 1994; Wilson et al., 2008) and research in young human adults have reported significant associations between fornix microstructure and place processing (Hodgetts et al., 2015; Postans et al., 2014). Specifically, given that the body stimuli studied here had no emotional traits and their relatively abstract nature, it is likely that these categories rely on considerable levels of attention/working memory and executive control (Bourbon-Teles et al., 2021; Jorge et al., 2018), functions that have also been previously attributed to the fornix and the hippocampus (Leszczynski, 2011; Nestor et al., 2007; Zahr et al., 2009). Similarly, previous evidence also indicates that short-term encoding of verbal categories relies on considerable levels of executive control and involvement of associated control networks (e.g., Jorge et al., 2018) which could explain the fornical predictive association.

Thus, it also important to consider that deficits in cognitive performance exhibited by the AD patients may also pertain to more general attributes of the 1-back tasks (and not just related to the type of visual stimuli per se). Nevertheless, false alarms were rare in the non-match trials.

Thus, our findings are also in keeping with previous influential accounts on early onset AD in that while A $\beta$  depositions constitute one of the earliest hallmarks of AD, subsequent neurodegeneration within the MTL structures are better predictive of the cognitive and clinical symptoms since overall, we report more tight/robust associations between fornix microstructural integrity and cognitive performance measures in the AD patient group (Figure 3) (Berron et al., 2020; Hanseeuw et al., 2019; Hardy & Allsop, 1991; Marks et al., 2017; Svenningsson et al., 2019). Accordingly, a complementary analysis also revealed an association between overall cognitive performance measures with fornix microstructure but not with cortical A $\beta$  burden. Nonetheless, it also important to acknowledge the statistical limitations of the present study which is only correlational by nature and based on a low study sample and the importance of prospective longitudinal studies in design and with larger study samples to more accurately determine the differential effects of cortical A $\beta$  burden and/or fornix microstructural impairments (or even an interaction-effect between both measures) to cognitive performance declines in early AD (e.g., as measured by 1-back working memory tasks for visual object categories).

There was no cross-sectional association between fornix FA and cortical A $\beta$  burden. One possibility is that the current study sample was not large enough to detect such effects. Some of the previous related studies who have reported associations between fornix microstructure and A $\beta$  burden still included larger samples than the current one (Brown et al., 2016; Chao et al., 2013) although others failed to report any associations at this level (e.g., Rabin et al., 2019). Second, it is possible that at early stages of the disease measures of cortical A $\beta$  load likely co-occur more directly with more ancient neuropathological measures such as tau phosphorylation/tangle formation rather than with fornix degeneration although it is possible that this level of association may become more visible at later stages of the disease with increasing fornix deterioration (Hanseeuw et al., 2019; Hardy & Allsop, 1991; Marks et al., 2017; Reitz, 2012). Indeed, it is observable in the current study that between-group differences in cortical A $\beta$  burden are considerably larger than that of fornix degeneration which could explain any lack of association between these two critical neuropathological measures.

In sum, our findings support contributions of cortical A $\beta$  burden and even into a larger extent of fornix microstructural changes to cognitive deficits in early AD beyond memory, namely deficits in the short-term/working memory maintenance of object categories. The fornix could serve as a new target region for future intervention studies (e.g., in deep brain stimulation studies) aiming to delay disease progressing and the onset of cognitive/clinical symptoms in early AD.

Prospective longitudinal studies with large study samples will be essential to achieve more robust and solid conclusions concerning the differential effects of cortical A $\beta$  burden and/or fornix microstructural changes to cognitive deficits in early AD (e.g., in visual working memory processes).

## ACKNOWLEDGMENTS

This work was supported by Grants Funded by Fundação para a Ciência e Tecnologia PAC–286 MEDPERSYST, POCI-01-0145-FEDER-016428, BIGDATIMAGE.CENTRO-01-0145-FEDER-000016, FCT/DSAIPA/DS/0041/2020, PTDC/PSI-GER/1326/2020 FCT/UIDB/4950 and FCT/UIDP/4950.

## CONFLICT OF INTEREST

The authors have no conflict of interest to declare.

## DATA AVAILABILITY STATEMENT

The data that support the findings of this study are available on request from the corresponding author. The data are not publicly available due to privacy or ethical restrictions.

## ORCID

Ricardo Martins  <https://orcid.org/0000-0001-7184-185X>

Miguel Castelo-Branco  <https://orcid.org/0000-0003-4364-6373>

## REFERENCES

Acosta-Cabronero, J., & Nestor, P. J. (2014). Diffusion tensor imaging in Alzheimer's disease: Insights into the limbic-diencephalic network and

- methodological considerations. *Frontiers in Aging Neuroscience*, 6, 266. <https://doi.org/10.3389/fnagi.2014.00266>
- Aggleton, J. P. (2012). Multiple anatomical systems embedded within the primate medial temporal lobe: Implications for hippocampal function. *Neuroscience & Biobehavioral Reviews*, 36, 1579–1596. <https://doi.org/10.1016/j.neubiorev.2011.09.005>
- Aggleton, J. P., Keith, A. B., Rawlins, J. N., Hunt, P. R., & Sahgal, A. (1992). Removal of the hippocampus and transection of the fornix produce comparable deficits on delayed non-matching to position by rats. *Behavioural Brain Research*, 52, 61–71. [https://doi.org/10.1016/s0166-4328\(05\)80325-0](https://doi.org/10.1016/s0166-4328(05)80325-0)
- Aggleton, J. P., O'Mara, S. M., Vann, S. D., Wright, N. F., Tsanov, M., & Erichsen, J. T. (2010). Hippocampal-anterior thalamic pathways for memory: Uncovering a network of direct and indirect actions. *European Journal of Neuroscience*, 3, 2292–2307. <https://doi.org/10.1111/j.14609568.2010.07251.x>
- Ashburner, J. (2007). A fast diffeomorphic image registration algorithm. *NeuroImage*, 38, 95–113. <https://doi.org/10.1016/j.neuroimage.2007.07.007>
- Barreto, J., Leuschner, A., Santos, F., & Sobral, M. (2008). Escala de Depressão Geriátrica [Geriatric depressive scale]. In C. Mendonça, C. Garcia, & M. Guerreiro (Eds.), *Grupo de Estudos de Envelhecimento cerebral e Demências [study group on brain aging and dementia]. Escalas e testes Na Demência [scales and tests in dementia]* (pp. 69–72). GEEDC.
- Berron, D., van Westen, D., Ossenkoppele, R., Strandberg, O., & Hansson, O. (2020). Medial temporal lobe connectivity and its associations with cognition in early Alzheimer's disease. *Brain*, 143, 1233–1248. <https://doi.org/10.1093/brain/awaa068>
- Bird, C. M., & Burgess, N. (2008). The hippocampus and memory: Insights from spatial processing. *Nature Reviews Neuroscience*, 9, 182–194. <https://doi.org/10.1038/nrn2335>
- Bourbon-Teles, J., Canário, N., Jorge, L., & Castelo-Branco, M. (2021). Frontoparietal microstructural damage mediates age-dependent working memory decline in face and body information processing: Evidence for dichotomic hemispheric bias mechanisms. *Neuropsychologia*, 151, 107726. <https://doi.org/10.1016/j.neuropsychologia.2020.107726>
- Brown, C. A., Johnson, N. F., Anderson-Mooney, A. J., Jicha, G. A., Shaw, L. M., Trojanowski, J. Q., Van Eldik, L. J., Schmitt, F. A., Smith, C. D., & Gold, B. T. (2016). Development, validation and application of a new fornix template for studies of aging and preclinical Alzheimer's disease. *NeuroImage: Clinical*, 13, 106–115. <https://doi.org/10.1016/j.nicl.2016.11.024>
- Bubb, E. J., Metzler-Baddeley, C., & Aggleton, J. P. (2018). The cingulum bundle: Anatomy, function, and dysfunction. *Neuroscience & Biobehavioral Reviews*, 92, 104–127. <https://doi.org/10.1016/j.neubiorev.2018.05.008>
- Buckley, M. J., Charles, D. P., Browning, P. G. F., & Gaffan, D. (2004). Learning and retrieval of concurrently presented spatial discrimination tasks: Role of the fornix. *Behavioral Neuroscience*, 118, 138–149. <https://doi.org/10.1037/0735-7044.118.1.138>
- Canário, N., Jorge, L., Loureiro Silva, M. F., Alberto Soares, M., & Castelo-Branco, M. (2016). Distinct preference for spatial frequency content in ventral stream regions underlying the recognition of scenes, faces, bodies and other objects. *Neuropsychologia*, 87, 110–119. <https://doi.org/10.1016/j.neuropsychologia.2016.05.010>
- Cassaday, H. J., & Rawlins, J. N. P. (1995). Fornix-fimbria section and working memory deficits in rats: Stimulus complexity and stimulus size. *Behavioral Neuroscience*, 109, 594–606. <https://doi.org/10.1037/0735-7044.109.4.594>
- Cattell, R. B. (1952). *Factor analysis*. Harper.
- Chao, L. L., Decarli, C., Kriger, S., Truran, D., Zhang, Y., Laxamana, J., Villeneuve, S., Jagust, W. J., Sanossian, N., Mack, W. J., Chui, H. C., & Weiner, M. W. (2013). Associations between white matter hyperintensities and  $\beta$  amyloid on integrity of projection, association, and limbic

- fiber tracts measured with diffusion tensor MRI. *PLoS One*, 8, e65175. <https://doi.org/10.1371/journal.pone.0065175>
- Cho, H., Choi, J. Y., Hwang, M. S., Kim, Y. J., Lee, H. M., Lee, H. S., Lee, J. H., Ryu, Y. H., Lee, M. S., & Lyoo, C. H. (2016). In vivo cortical spreading pattern of tau and amyloid in the Alzheimer disease spectrum. *Annals of Neurology*, 80, 247–258. <https://doi.org/10.1002/ana.24711>
- de Toledo-Morrell, L., Dickerson, B., Sullivan, M. P., Spanovic, C., Wilson, R., & Bennett, D. A. (2000). Hemispheric differences in hippocampal volume predict verbal and spatial memory performance in patients with Alzheimer's disease. *Hippocampus*, 10, 136–142. [https://doi.org/10.1002/\(SICI\)1098-1063\(2000\)10:2<136::AID-HIPO2>3.0.CO;2-J](https://doi.org/10.1002/(SICI)1098-1063(2000)10:2<136::AID-HIPO2>3.0.CO;2-J)
- de Winter, J. C., Dodou, D., & Wieringa, P. A. (2009). Exploratory factor analysis with small sample sizes. *Multivariate Behavioral Research*, 44, 147–181. <https://doi.org/10.1080/00273170902794206>
- Dennis, N. A., Hayes, S. M., Prince, S. E., Madden, D. J., Huettel, S. A., & Cabeza, R. (2008). Effects of aging on the neural correlates of successful item and source memory encoding. *Journal of Experimental Psychology: Learning, Memory, and Cognition*, 34, 791–808. <https://doi.org/10.1037/0278-7393.34.4.791>
- Desikan, R. S., Cabral, H. J., Hess, C. P., Dillon, W. P., Glastonbury, C. M., Weiner, M. W., Schmansky, N. J., Greve, D. N., Salat, D. H., Buckner, R. L., & Fischl, B. (2009). Automated MRI measures identify individuals with mild cognitive impairment and Alzheimer's disease. *Brain*, 132, 2048–2057. <https://doi.org/10.1093/brain/awp123>
- Devanand, D. P., Bansal, R., Liu, J., Hao, X., Pradhaban, G., & Peterson, B. S. (2012). MRI hippocampal and entorhinal cortex mapping in predicting conversion to Alzheimer's disease. *NeuroImage*, 60, 1622–1629. <https://doi.org/10.1016/j.neuroimage.2012.01.075>
- Douet, V., & Chang, L. (2015). Fornix as an imaging marker for episodic memory deficits in healthy aging and in various neurological disorders. *Frontiers in Aging Neuroscience*, 6, 343. <https://doi.org/10.3389/fnagi.2014.00343>
- Ebner, N. C., Riediger, M., & Lindenberger, U. (2010). FACES—a database of facial expressions in young, middle-aged, and older women and men: development and validation. *Behavior Research Methods*, 42, 351–362. <https://doi.org/10.3758/BRM.42.1.351>
- Edmonds, E. C., Bangen, K. J., Delano-Wood, L., Nation, D. A., Furst, A. J., Salmon, D. P., & Bondi, M. W. (2016). Patterns of cortical and subcortical amyloid burden across stages of preclinical Alzheimer's disease. *The Journal of the International Neuropsychological Society*, 22, 978–990. <https://doi.org/10.1017/S1355617716000928>
- Ezzyat, Y., & Olson, I. R. (2008). The medial temporal lobe and visual working memory: Comparisons across tasks, delays, and visual similarity. *Cognitive, Affective, & Behavioral Neuroscience*, 8, 32–40. <https://doi.org/10.3758/cabn.8.1.32>
- Fletcher, E., Raman, M., Huebner, P., Liu, A., Mungas, D., Carmichael, O., & De Carli, C. (2013). Loss of fornix white matter volume as a predictor of cognitive impairment in cognitively normal elderly individuals. *JAMA Neurology*, 70, 1389–1395. <https://doi.org/10.1001/jamaneurol.2013.3263>
- Folstein, M. F., Folstein, S. E., & McHugh, P. R. (1975). "Mini-mental state". A practical method for grading the cognitive state of patients for the clinician. *Journal of Psychiatric Research*, 12, 189–198. [https://doi.org/10.1016/0022-3956\(75\)90026-6](https://doi.org/10.1016/0022-3956(75)90026-6)
- Freitas, S., Simões, M. R., Alves, L., & Santana, I. (2013). Montreal cognitive assessment: Validation study for mild cognitive impairment and Alzheimer disease. *Alzheimer Disease & Associated Disorders*, 27, 37–43. <https://doi.org/10.1097/WAD.0b013e3182420bfe>
- Freitas, S., Simões, M. R., Alves, L., & Santana, I. (2015). The relevance of sociodemographic and health variables on MMSE normative data. *Applied Neuropsychology. Adult*, 22, 311–319. <https://doi.org/10.1080/23279095.2014.926455>
- Frisoni, G. B., Fox, N. C., Jack, C. R., Jr., Scheltens, P., & Thompson, P. M. (2010). The clinical use of structural MRI in Alzheimer disease. *Nature Reviews Neurology*, 6, 67–77. <https://doi.org/10.1038/nrneurol.2009.215>
- Gaffan, D. (1994). Scene-specific memory for objects: A model of episodic memory impairment in monkeys with fornix transection. *Journal of Cognitive Neuroscience*, 6, 305–320. <https://doi.org/10.1162/jocn.1994.6.4.305>
- Galani, R., Obis, S., Coutureau, E., Jarrard, L., & Cassel, J. C. (2002). A comparison of the effects of fimbria-fornix, hippocampal, or entorhinal cortex lesions on spatial reference and working memory in rats: Short versus long postsurgical recovery period. *Neurobiology of Learning and Memory*, 77, 1–16. <https://doi.org/10.1006/nlme.2000.3998>
- Ginó, S., Mendes, T., Ribeiro, F., Mendonça, A., Guerreiro, M., & Garcia, C. (2008). Escala de Queixas de Memória [subjective memory complaints]. In C. Mendonça, C. Garcia, & M. Guerreiro (Eds.), *Grupo de Estudos de Envelhecimento Cerebral e Demências [Study Group on Brain Aging and Dementia]. Escalas e Testes Na Demência [Scales and Tests in Dementia]* (pp. 116–120). GEECD.
- Grady, C. L., McIntosh, A. R., Horwitz, B., Maisog, J. M., Ungerleider, L. G., Mentis, M. J., Pietrini, P., Schapiro, M. B., & Haxby, J. V. (1995). Age-related reductions in human recognition memory due to impaired encoding. *Science*, 269, 218–221. <https://doi.org/10.1126/science.7618082>
- Guerreiro, M. (1998). *Contributo da neuropsicologia para o estudo das demências [contribution of neuropsychology to the study of dementia]*. University of Lisbon.
- Hannula, D. E., Tranel, D., & Cohen, N. J. (2006). The long and the short of it: Relational memory impairments in amnesia, even at short lags. *Journal of Neuroscience*, 26, 8352–8359. <https://doi.org/10.1523/JNEUROSCI.5222-05.2006>
- Hanseeuw, B. J., Betensky, R. A., Jacobs, H. I. L., Schultz, A. P., Sepulcre, J., Becker, J. A., Cosio, D. M. O., Farrell, M., Quiroz, Y. T., Mormino, E. C., Buckley, R. F., Papp, K. V., Amariglio, R. A., Dewachter, I., Ivanou, A., Huijbers, W., Hedden, T., Marshall, G. A., Chhatwal, J. P., ... Johnson, K. (2019). Association of amyloid and tau with cognition in preclinical Alzheimer disease: A longitudinal study. *JAMA Neurology*, 76, 915–924. <https://doi.org/10.1001/jamaneurol.2019.1424>
- Hardy, J., & Allsop, D. (1991). Amyloid deposition as the central event in the aetiology of Alzheimer's disease. *Trends in Pharmacological Sciences*, 12, 383–388. [https://doi.org/10.1016/0165-6147\(91\)90609-v](https://doi.org/10.1016/0165-6147(91)90609-v)
- Hodgetts, C. J., Postans, M., Shine, J. P., Jones, D. K., Lawrence, A. D., & Graham, K. S. (2015). Dissociable roles of the inferior longitudinal fasciculus and fornix in face and place perception. *eLife*, 4, e07902. <https://doi.org/10.7554/eLife.07902>
- Huang, H., Fan, X., Weiner, M., Martin-Cook, K., Xiao, G., Davis, J., Devous, M., Rosenberg, R., & Diaz-Arrastia, R. (2012). Distinctive disruption patterns of white matter tracts in Alzheimer's disease with full diffusion tensor characterization. *Neurobiology of Aging*, 33, 2029–2045. <https://doi.org/10.1016/j.neurobiolaging.2011.06.027>
- Irfanoglu, M. O., Walker, L., Sarlls, J., Marenco, S., & Pierpaoli, C. (2012). Effects of image distortions originating from susceptibility variations and concomitant fields on diffusion MRI tractography results. *NeuroImage*, 6, 275–288. <https://doi.org/10.1016/j.neuroimage.2012.02.054>
- Jeurissen, B., Leemans, A., Jones, D. K., Tournier, J. D., & Sijbers, J. (2011). Probabilistic fiber tracking using the residual bootstrap with constrained spherical deconvolution. *Human Brain Mapping*, 32, 461–479. <https://doi.org/10.1002/hbm.21032>
- Jolliffe, I. (1986). *Principal component analysis*. Springer.
- Jorge, L., Canário, N., Castelhamo, J., & Castelo-Branco, M. (2018). Processing of performance-matched visual object categories: Faces and places are related to lower processing load in the frontoparietal executive network than other objects. *European Journal of Neuroscience*, 47, 938–946. <https://doi.org/10.1111/ejn.13892>

- Jorge, L., Martins, R., Canário, N., Xavier, C., Abrunhosa, A., Santana, I., & Castelo-Branco, M. (2021). Investigating the spatial associations between amyloid- $\beta$  deposition, grey matter volume, and neuroinflammation in Alzheimer's disease. *Journal of Alzheimer's Disease*, *80*, 113–132. <https://doi.org/10.3233/JAD-200840>
- Kantarci, K. (2014). Fractional anisotropy of the fornix and hippocampal atrophy in Alzheimer's disease. *Frontiers in Aging Neuroscience*, *6*, 316. <https://doi.org/10.3389/fnagi.2014.00316>
- Kensinger, E. A., Shearer, D. K., Locascio, J. J., Growdon, J. H., & Corkin, S. (2003). Working memory in mild Alzheimer's disease and early Parkinson's disease. *Neuropsychology*, *17*, 230–239. <https://doi.org/10.1037/0894-4105.17.2.230>
- Kikinis, R., Pieper, S. D., & Vosburgh, K. G. (2014). 3D slicer: A platform for subject-specific image analysis, visualization, and clinical support. In F. Jolesz (Ed.), *Intraoperative imaging and image-guided therapy*. Springer. [https://doi.org/10.1007/978-1-4614-7657-3\\_19](https://doi.org/10.1007/978-1-4614-7657-3_19)
- Köhler, S., Black, S. E., Sinden, M., Szekely, C., Kidron, D., Parker, J. L., Foster, J. K., Moscovitch, M., Winocour, G., Szalai, J. P., & Bronskill, M. J. (1998). Memory impairments associated with hippocampal versus parahippocampal-gyrus atrophy: An MR volumetry study in Alzheimer's disease. *Neuropsychologia*, *36*, 901–914. [https://doi.org/10.1016/s0028-3932\(98\)00017-7](https://doi.org/10.1016/s0028-3932(98)00017-7)
- Lawton, M. P., & Brody, E. M. (1969). Assessment of older people: Self-maintaining and instrumental activities of daily living. *Gerontologist*, *9*, 179–186.
- Lee, D. Y., Fletcher, E., Carmichael, O. T., Singh, B., Mungas, D., Reed, B., Martinez, O., Buonocore, M. H., Persianinova, M., & Decarli, C. (2012). Sub-regional hippocampal injury is associated with fornix degeneration in Alzheimer's disease. *Frontiers in Aging Neuroscience*, *4*, 1. <https://doi.org/10.3389/fnagi.2012.00001>
- Leemans, A., Jeurissen, B., Sijbers, J., & Jones, D. K. (2009). ExploreDTI: A graphical toolbox for processing, analyzing, and visualizing diffusion MR data. *Proceedings of the International Society for Magnetic Resonance in Medicine*.
- Leemans, A., & Jones, D. K. (2009). The B-matrix must be rotated when correcting for subject motion in DTI data. *Magnetic Resonance in Medicine*, *61*, 1336–1349. <https://doi.org/10.1002/mrm.21890>
- Leszczynski, M. (2011). How does hippocampus contribute to working memory processing? *Frontiers in Human Neuroscience*, *5*, 168. <https://doi.org/10.3389/fnhum.2011.00168>
- Madureira, S., & Verdelho, A. (2008). Escala de Atividades Instrumentais de Vida Diária [instrumental activities of daily living]. In C. Mendonça, C. Garcia, & M. Guerreiro (Eds.), *Grupo de Estudos de Envelhecimento cerebral e Demências [study group on brain aging and dementia]*. Escalas e testes Na Demência [scales and tests in dementia] (pp. 121–124). GEECD.
- Markowska, A. L., Olton, D. S., Murray, E. A., & Gaffan, D. (1989). A comparative analysis of the role of fornix and cingulate cortex in memory: Rats. *Experimental Brain Research*, *74*, 187–201. <https://doi.org/10.1007/BF00248292>
- Marks, S. M., Lockhart, S. N., Baker, S. L., & Jagust, W. J. (2017). Tau and  $\beta$ -amyloid are associated with medial temporal lobe structure, function, and memory encoding in Normal aging. *Journal of Neuroscience*, *37*, 3192–3201. <https://doi.org/10.1523/JNEUROSCI.3769-16.2017>
- McKhann, G. M., Knopman, D. S., Chertkow, H., Hyman, B. T., Jack, C. R., Jr., Kawas, C. H., Klunk, W. E., Koroshetz, W. J., Manly, J. J., Mayeux, R., Mohs, R. C., Morris, J. C., Rossor, M. N., Scheltens, P., Carrillo, M. C., Thies, B., Weintraub, S., & Phelps, C. H. (2011). The diagnosis of dementia due to Alzheimer's disease: Recommendations from the National Institute on Aging-Alzheimer's Association workgroups on diagnostic guidelines for Alzheimer's disease. *Alzheimer's & Dementia*, *7*, 263–269. <https://doi.org/10.1016/j.jalz.2011.03.005>
- Metzler-Baddeley, C., Jones, D. K., Belaroussi, B., Aggleton, J. P., & O'Sullivan, M. J. (2011). Frontotemporal connections in episodic memory and aging: A diffusion MRI tractography study. *Journal of Neuroscience*, *31*, 13236–13245. <https://doi.org/10.1523/JNEUROSCI.2317-11.2011>
- Metzler-Baddeley, C., Mole, J. P., Sims, R., Fasano, F., Evans, J., Jones, D. K., Aggleton, J. P., & Baddeley, R. J. (2019). Fornix white matter glia damage causes hippocampal gray matter damage during age-dependent limbic decline. *Scientific Reports*, *9*, 1060. <https://doi.org/10.1038/s41598-018-37658-5>
- Metzler-Baddeley, C., O'Sullivan, M. J., Bells, S., Pasternak, O., & Jones, D. K. (2012). How and how not to correct for CSF-contamination in diffusion MRI. *NeuroImage*, *59*, 1394–1403. <https://doi.org/10.1016/j.neuroimage.2011.08.043>
- Mielke, M. M., Okonkwo, O. C., Oishi, K., Mori, S., Tighe, S., Miller, M. I., Ceritoglu, C., Brown, T., Albert, M., & Lyketsos, C. G. (2012). Fornix integrity and hippocampal volume predict memory decline and progression to Alzheimer's disease. *Alzheimer's & Dementia*, *8*, 105–113. <https://doi.org/10.1016/j.jalz.2011.05.2416>
- Morris, J. C. (1993). The clinical dementia rating (CDR): Current version and scoring rules. *Neurology*, *43*, 2412–2414. <https://doi.org/10.1212/wnl.43.11.2412-a>
- Nasreddine, Z. S., Phillips, N. A., Bédirian, V., Charbonneau, S., Whitehead, V., Collin, I., Cummings, J. L., & Chertkow, H. (2005). The Montreal cognitive assessment, MoCA: A brief screening tool for mild cognitive impairment. *Journal of the American Geriatrics Society*, *53*, 695–699. <https://doi.org/10.1111/j.1532-5415.2005.53221.x>
- Nestor, P. G., Kubicki, M., Kuroki, N., Gurrera, R. J., Niznikiewicz, M., Shenton, M. E., & McCarley, R. W. (2007). Episodic memory and neuroimaging of hippocampus and fornix in chronic schizophrenia. *Psychiatry Research*, *155*, 21–28. <https://doi.org/10.1016/j.psychres.2006.12.020>
- Nichols, E. A., Kao, Y. C., Verfaellie, M., & Gabrieli, J. D. (2006). Working memory and long-term memory for faces: Evidence from fMRI and global amnesia for involvement of the medial temporal lobes. *Hippocampus*, *16*, 604–616. <https://doi.org/10.1002/hipo.20190>
- Oishi, K., & Lyketsos, C. G. (2014). Alzheimer's disease and the fornix. *Frontiers in Aging Neuroscience*, *6*, 241. <https://doi.org/10.3389/fnagi.2014.00241>
- Oliva, A., & Torralba, A. (2001). Modeling the shape of the scene: A holistic representation of the spatial envelope. *International Journal of Computer Vision*, *42*, 145–175. <https://doi.org/10.1023/A:1011139631724>
- Oliveira, F. P. M., Moreira, A. P., de Mendonça, A., Verdelho, A., Xavier, C., Barroca, D., Rio, J., Cardoso, E., Cruz, Á., Abrunhosa, A., & Castelo-Branco, M. (2018). Can 11C-PiB-PET relative delivery R1 or 11C-PiB-PET perfusion replace 18F-FDG-PET in the assessment of brain neurodegeneration? *Journal of Alzheimer's Disease*, *65*, 89–97. <https://doi.org/10.3233/JAD-180274>
- Olson, I. R., Moore, K. S., Stark, M., & Chatterjee, A. (2006). Visual working memory is impaired when the medial temporal lobe is damaged. *Journal of Cognitive Neuroscience*, *18*, 1087–1097. <https://doi.org/10.1162/jocn.2006.18.7.1087>
- Petersen, R. C., Jack, C. R., Jr., Xu, Y. C., Waring, S. C., O'Brien, P. C., Smith, G. E., Ivnik, R. J., Tangalos, E. G., Boeve, B. F., & Kokmen, E. (2000). Memory and MRI-based hippocampal volumes in aging and AD. *Neurology*, *54*, 581–587. <https://doi.org/10.1212/wnl.54.3.581>
- Pierpaoli, C., Barnett, A., Pajevic, S., Chen, R., Penix, L. R., Virts, A., & Basser, P. (2001). Water diffusion changes in Wallerian degeneration and their dependence on white matter architecture. *NeuroImage*, *13*, 1174–1185. <https://doi.org/10.1006/nimg.2001.0765>
- Postans, M., Hodgetts, C. J., Mundy, M. E., Jones, D. K., Lawrence, A. D., & Graham, K. S. (2014). Interindividual variation in fornix microstructure and macrostructure is related to visual discrimination accuracy for scenes but not faces. *Journal of Neuroscience*, *34*, 12121–12126. <https://doi.org/10.1523/jneurosci.0026-14.2014>
- Preacher, K. J., & MacCallum, R. C. (2002). Exploratory factor analysis in behavior genetics research: Factor recovery with small sample sizes. *Behavior Genetics*, *32*, 153–161. <https://doi.org/10.1023/a:1015210025234>



- Price, J. C., Klunk, W. E., Lopresti, B. J., Lu, X., Hoge, J. A., Ziolkowski, S. K., Holt, D. P., Meltzer, C. C., DeKosky, S. T., & Mathis, C. A. (2005). Kinetic modeling of amyloid binding in humans using PET imaging and Pittsburgh compound-B. *Journal of Cerebral Blood Flow & Metabolism*, 25, 1528–1547. <https://doi.org/10.1038/sj.jcbfm.9600146>
- Rabin, J. S., Perea, R. D., Buckley, R. F., Johnson, K. A., Sperling, R. A., & Hedden, T. (2019). Synergism between fornix microstructure and beta amyloid accelerates memory decline in clinically normal older adults. *Neurobiology of Aging*, 81, 38–46. <https://doi.org/10.1016/j.neurobiolaging.2019.05.005>
- Reitz, C. (2012). Alzheimer's disease and the amyloid cascade hypothesis: A critical review. *International Journal of Alzheimer's Disease*, 2012, 369808. <https://doi.org/10.1155/2012/369808>
- Schmand, B., Jonker, C., Hooijer, C., & Lindeboom, J. (1996). Subjective memory complaints may announce dementia. *Neurology*, 46, 121–125. <https://doi.org/10.1212/wnl.46.1.121>
- Soares, J. M., Marques, P., Alves, V., & Sousa, N. (2013). A hitchhiker's guide to diffusion tensor imaging. *Frontiers in Neuroscience*, 7, 31. <https://doi.org/10.3389/fnins.2013.00031>
- Sperling, R. A., Dickerson, B. C., Pihlajamaki, M., Vannini, P., LaViolette, P. S., Vitolo, O. V., Hedden, T., Becker, J. A., Rentz, D. M., Selkoe, D. J., & Johnson, K. A. (2010). Functional alterations in memory networks in early Alzheimer's disease. *Neuromolecular Medicine*, 12, 27–43. <https://doi.org/10.1007/s12017-009-8109-7>
- Svenningsson, A. L., Stomrud, E., Insel, P. S., Mattsson, N., Palmqvist, S., & Hansson, O. (2019).  $\beta$ -Amyloid pathology and hippocampal atrophy are independently associated with memory function in cognitively healthy elderly. *Scientific Reports*, 9, 11180. <https://doi.org/10.1038/s41598-019-47638-y>
- Sziklas, V., & Petrides, M. (2002). Effects of lesions to the hippocampus or the fornix on allocentric conditional associative learning in rats. *Hippocampus*, 12, 543–550. <https://doi.org/10.1002/hipo.10030>
- Thiebaut de Schotten, M., Dell'Acqua, F., Forkel, S. J., Simmons, A., Vergani, F., Murphy, D. G., & Catani, M. (2011). A lateralized brain network for visuospatial attention. *Nature Neuroscience*, 14, 1245–1246. <https://doi.org/10.1038/nn.2905>
- Thoma, P., Soria Bauser, D., & Suchan, B. (2013). BESST (Bochum emotional stimulus set)--a pilot validation study of a stimulus set containing emotional bodies and faces from frontal and averted views. *Psychiatry Research*, 209, 98–109. <https://doi.org/10.1016/j.psychres.2012.11.012>
- Tournier, J. D., Calamante, F., & Connelly, A. (2007). Robust determination of the fibre orientation distribution in diffusion MRI: Non-negativity constrained super-resolved spherical deconvolution. *NeuroImage*, 35, 1459–1472. <https://doi.org/10.1016/j.neuroimage.2007.02.016>
- Tournier, J. D., Calamante, F., Gadian, D. G., & Connelly, A. (2004). Direct estimation of the fiber orientation density function from diffusion-weighted MRI data using spherical deconvolution. *NeuroImage*, 23, 1176–1185. <https://doi.org/10.1016/j.neuroimage.2004.07>
- Tzourio-Mazoyer, N., Landeau, B., Papathanassiou, D., Crivello, F., Etard, O., Delcroix, N., Mazoyer, B., & Joliot, M. (2002). Automated anatomical labeling of activations in SPM using a macroscopic anatomical parcellation of the MNI MRI single-subject brain. *NeuroImage*, 15, 273–289. <https://doi.org/10.1006/nimg.2001.0978>
- Warren, D. E., Duff, M. C., Cohen, N. J., & Tranel, D. (2014). Hippocampus contributes to the maintenance but not the quality of visual information over time. *Learning and Memory*, 22, 6–10. <https://doi.org/10.1101/lm.037127.114>
- Warren, D. E., Duff, M. C., Jensen, U., Tranel, D., & Cohen, N. J. (2012). Hiding in plain view: Lesions of the medial temporal lobe impair online representation. *Hippocampus*, 22, 1577–1588. <https://doi.org/10.1002/hipo.21000>
- Willenbockel, V., Sadr, J., Fiset, D., Horne, G. O., Gosselin, F., & Tanaka, J. W. (2010). Controlling low-level image properties: The SHINE toolbox. *Behavior Research Methods*, 42, 671–684. <https://doi.org/10.3758/BRM.42.3.671>
- Wilson, C. R. E., Baxter, M. G., Easton, A., & Gaffan, D. (2008). Addition of fornix transection to frontal-temporal disconnection increases the impairment in object-in-place memory in macaque monkeys. *European Journal of Neuroscience*, 27, 1814–1822. <https://doi.org/10.1111/j.1460-9568.2008.06140.x>
- Yesavage, J. A., Brink, T. L., Rose, T. L., Lum, O., Huang, V., Adey, M., & Leirer, V. O. (1982). Development and validation of a geriatric depression screening scale: A preliminary report. *Journal of Psychiatric Research*, 17, 37–49. [https://doi.org/10.1016/0022-3956\(82\)90033-4](https://doi.org/10.1016/0022-3956(82)90033-4)
- Zahr, N. M., Rohlfing, T., Pfefferbaum, A., & Sullivan, E. V. (2009). Problem solving, working memory, and motor correlates of association and commissural fiber bundles in normal aging: A quantitative fiber tracking study. *NeuroImage*, 44, 1050–1062. <https://doi.org/10.1016/j.neuroimage.2008.09.046>
- Zhang, Y., Hedo, R., Rivera, A., Rull, R., Richardson, S., & Tu, X. M. (2019). Post hoc power analysis: Is it an informative and meaningful analysis? *General Psychiatry*, 32, e100069. <https://doi.org/10.1136/gpsych-2019-100069>
- Zhuang, L., Sachdev, P. S., Trollor, J. N., Reppermund, S., Kochan, N. A., Brodaty, H., & Wen, W. (2013). Microstructural white matter changes, not hippocampal atrophy, detect early amnesic mild cognitive impairment. *PLoS One*, 8, e58887. <https://doi.org/10.1371/journal.pone.0058887>
- Zokaei, N., & Husain, M. (2019). Working memory in Alzheimer's disease and Parkinson's disease. *Current Topics in Behavioral Neurosciences*, 41, 325–344. [https://doi.org/10.1007/7854\\_2019\\_103](https://doi.org/10.1007/7854_2019_103)

**How to cite this article:** Bourbon-Teles, J., Jorge, L., Canário, N., Martins, R., Santana, I., & Castelo-Branco, M. (2022). Associations between cortical  $\beta$ -amyloid burden, fornix microstructure and cognitive processing of faces, places, bodies and other visual objects in early Alzheimer's disease. *Hippocampus*, 1–13. <https://doi.org/10.1002/hipo.23493>